Available online at www.sciencedirect.com
ScienceDirect
European Journal of Mechanics B/Fluids 27 (2008) 96–109

Large-amplitude steady rotational water waves

Joy Ko [a,*], Walter Strauss [b]

[a] *Department of Mathematics, Brown University, Providence, RI 02912, USA*
[b] *Lefschetz Center for Dynamical Systems and Department of Mathematics, Brown University, Providence, RI 02912, USA*

Received 5 December 2006; received in revised form 6 April 2007; accepted 7 April 2007

Available online 18 May 2007

Abstract

Two-dimensional, finite-depth periodic water waves with general vorticity and large amplitude are computed. The mathematical formulation and numerical method that allow us to compute a continuum of such waves with arbitrary vorticity are described. The problems of whether extreme waves exist, where their stagnation points occur, and what qualitative features such waves possess are addressed here with particular emphasis on constant vorticity.

Keywords: Vorticity; Rotational water waves; Extreme waves; Stagnation

1. Introduction

Evidence from experimental studies shows that qualitative features of water waves can be greatly affected by the presence of vorticity. However, numerical studies on rotational water waves have mostly been restricted to the simplified setting of constant vorticity. These studies have consistently shown that features such as the shape of the wave, the amplitude of the crest, and the presence of eddies differ from those found in the irrotational setting. There may be "extreme" waves that contain points of stagnation; they indicate the possibility of eddies or of overhanging crests. The irrotational case is the only one for which there is a complete picture of the "extreme" wave, that is, a wave with a stagnation point. This is the Stokes' wave, for which the only point of stagnation is the crest with an angle measuring 120°. Theoretical work concerning extreme rotational waves is quite sparse.

In the present work, we compute families of periodic water waves with general vorticity and large amplitude. The vorticity does not have to be constant; it is completely arbitrary. Our calculations make no shallowness or small-amplitude approximation. We do assume that the water is incompressible and inviscid without surface tension, lies over a flat bottom, and is acted upon by gravity g. We assume that the waves are two-dimensional, periodic and of permanent form. Then the only remaining free parameters are the period $2L$, the Bernoulli constant Q, the relative mass flux p_0, the speed c of the wave, and of course the vorticity function $\gamma(\cdot)$. The average depth d is determined implicitly in terms of the other parameters. We treat Q as a bifurcation parameter, thereby generating a one-parameter family of waves, for each choice of the other parameters.

* Corresponding author.
E-mail address: joyko@math.brown.edu (J. Ko).

0997-7546/$ – see front matter
doi:10.1016/j.euromechflu.2007.04.004

Our principal aim is to compare waves with different vorticities, especially with regard to the possibility of extreme waves with stagnation points. We are interested to see what these extreme waves look like and where the stagnation points are located. Key conclusions that are reached from our computations in the case of constant vorticity are as follows:

(1) There can be stagnation, not only at the crest, but also at the point on the bottom directly below the crest.
(2) These are the only two possibilities for a first stagnation point.
(3) The shapes of the streamlines of the extreme waves depend on the vorticity.
(4) Furthermore, in case the vorticity is variable, there can also be stagnation points inside the fluid.

There is of course a huge literature concerning irrotational waves, especially in various small-amplitude and shallow-water approximations. In case the vorticity ω is a *constant*, one can introduce a pseudo-stream function that is a harmonic function, in analogy with the irrotational case. Thus the Euler equations can be converted via the Cauchy integral theorem to a boundary-integral formulation. This formulation is relatively easy to solve numerically. The first to use this approach were Simmen and Saffman in [1] who considered periodic waves with infinite depth and Da Silva and Peregrine in [2] who treated periodic waves with finite depth. Da Silva and Peregrine showed that eddies can form at the finite bottom directly below the crest if the vorticity is positive and large enough. In case the vorticity is negative, an extreme wave can form with stagnation at the crest but it does not have the same shape as in the irrotational case. Their key paper clearly shows that vorticity can have a profound effect on the shape of the wave.

Using the same method, Vanden-Broeck in [3,4] and Okamoto and Shoji in [5] computed various families of solitary waves with finite depth and constant vorticity, obtaining results consistent with those of Da Silva and Peregrine. Miroshnikov in [6] also considered solitary waves using basically the same formulation. However, in his work the water has to be shallow and the numerical method is based on several approximations including an expansion in powers of the depth. As Da Silva and Peregrine did, Miroshnikov found eddies forming at the bottom if the vorticity is positive, but, in direct contradiction to the results of both Da Silva and Peregrine and Vanden-Broeck, he also found eddies forming near the crest.

A few papers have dealt with the case of *variable vorticity*. Dalrymple in [7] used a method based on the Dubreil-Jacotin transformation (DJ, see below), which permits the treatment of an arbitrary vorticity distribution. In fact, Dubreil-Jacotin [8] had been the first to provide any theoretical analysis of waves with general vorticities. Dalrymple specified all the physical constants and therefore he computed only particular examples in each run. He computed just two particular examples in detail, one with constant vorticity and one with a vorticity satisfying a power law.

Thomas in [9] also used the Dubreil-Jacotin method similarly to Dalrymple, computing individual waves, but included a background current and performed the computation using truncated Fourier modes. Solitary waves in the presence of a background current had been considered earlier by [10]. Comparing his numerical results with experimental data, Thomas' key conclusion was that the vorticity has a major influence on the nature of the wave.

Swan, Cummins and James in [11] undertook an experimental and numerical study of time-dependent waves propagating on a strongly sheared current with a nonconstant vorticity distribution. They found, experimentally, that a negative vorticity distribution can have several main effects on the gross appearance of a wave. It may produce increased wave amplitude. There may be greater crest-trough asymmetry (with a broader trough and a sharper crest). The wave may be steeper than in the irrotational case and thus the local acceleration of the water particles can be greater. Even if the vorticity is confined to the upper layers of the water, the flow is modified over the entire water depth. (We remark that what SCJ call "negatively sheared" is what we call "positive vorticity", and vice-versa.)

In this paper we follow the bifurcating curve using the parameter Q, after having fixed the relative mass flux p_0 and the period $2L$. We do not use truncated Fourier modes, nor shallow water or small amplitude approximations. Instead, we solve the fully elliptic system that results from the DJ transformation along the bifurcating curve, using standard finite differencing and nonlinear solvers, as well as the efficient numerical continuation library TRILINOS.

In Section 2 we present the theoretical background of the problem, including the DJ transformation and a summary of known mathematical results, especially those that concern the stagnation points. In Section 3 we describe our numerical method, including discussions of the numerical bifurcation and continuation procedures. In Section 4 we present the results of our simulations in the case of constant vorticity. There are three natural regimes, depending on whether the vorticity is sub-irrotational, supercritical, or in between. We conclude Section 4 with one instance of a

variable vorticity distribution which yields an internal point of stagnation. A much more extensive discussion of the variable vorticity case will follow in a subsequent paper.

2. Mathematical background

To describe steady periodic 2D water waves it suffices to consider a cross section of the flow that is perpendicular to the crest line. Choose Cartesian coordinates (x, y) with the y-axis pointing vertically upwards and the x-axis being the direction of wave propagation, with the origin located on the mean water level. Let $(u(t, x, y),\ v(t, x, y))$ be the velocity field of the flow, let $\{y = -d\}$ for some $d > 0$ be the flat bed, and let $S = \{y = \eta(t, x)\}$ be the water's free surface. The Euler equations are

$$u_x + v_y = 0, \quad u_t + uu_x + vu_y = -P_x, \quad v_t + uv_x + vv_y = -P_y - g, \tag{2.1}$$

where $P(t, x, y)$ denotes the pressure and g is the gravitational constant of acceleration. The free surface decouples the motion of the water from that of the air so that $P = P_{\text{atm}}$ on S, where P_{atm} is the atmospheric pressure and the surface tension is assumed to be negligible. Moreover, since the same particles always form the free surface, we have $v = \eta_t + u\eta_x$ on S. Similarly, $v = 0$ on $y = -d$. In this paper we assume that the flow is periodic, in the sense that the velocity field (u, v), the pressure P and the free surface η all have period (wavelength) $2L$ in the x-variable.

For steady periodic waves with wave speed $c > 0$ the (x, t)-dependence of the free surface, of the pressure and of the velocity field has the form $x - ct$. The incompressibility condition enables us to introduce a stream function $\psi(x, y)$ defined up to a constant by

$$\psi_x = -v, \qquad \psi_y = u - c.$$

Thus

$$\Delta\psi = -\omega,$$

where $\omega = v_x - u_y$ is the vorticity. The Euler equations (2.1) imply that ψ and ω have parallel gradients and the same level sets and are functionally dependent. If the steady wave satisfies the condition $u < c$ throughout the fluid, this functional dependence is global; that is, there exists a function γ, called the *vorticity function*, such that

$$\omega = \gamma(\psi)$$

throughout the fluid. Proofs of this statement and the following ones are either well known or can be found in [12]. Therefore the governing equations can be reformulated in the moving frame as

$$\begin{aligned}
&\Delta\psi = -\gamma(\psi) \quad \text{in } \{-d < y < \eta(x)\},\\
&|\nabla\psi|^2 + 2g(y + d) = Q \quad \text{on } \{y = \eta(x)\},\\
&\psi = 0 \quad \text{on } \{y = \eta(x)\},\\
&\psi = -p_0 \quad \text{on } \{y = -d\},
\end{aligned}$$

where

$$p_0 = \int_{-d}^{\eta(x)} (u - c)\, dy < 0$$

is the *relative mass flux* and is independent of x. The nonlinear boundary condition at $y = \eta(x)$ is an expression of Bernoulli's law, the *Bernoulli constant* Q being given by $Q = 2(E + gd)$, where E is the hydraulic head of the flow. We assume that

$$u < c \quad \text{throughout the fluid.} \tag{2.2}$$

Since the function ψ is constant on the free surface $S = \{y = \eta(x)\}$ as well as on the flat bed $y = -d$, it is natural to introduce the new independent variables

$$q = x, \qquad p = -\psi(x, y).$$

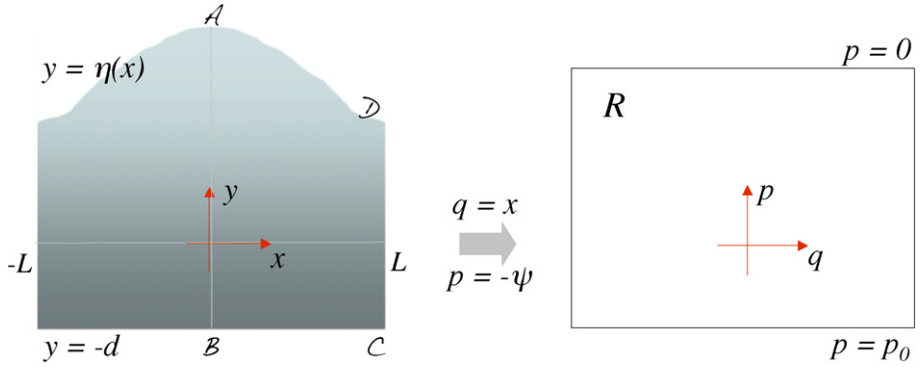

Fig. 1. Dubreil-Jacotin (DJ) transformation.

This is the Dubreil-Jacotin transformation [DJ], as illustrated by Fig. 1.

It has the effect of transforming the free boundary problem into the boundary value problem

$$\begin{cases} (1+h_q^2)h_{pp} - 2h_p h_q h_{pq} + h_p^2 h_{qq} = -\gamma(-p)h_p^3 & \text{in } R, \\ 1 + h_q^2 + (2gh - Q)h_p^2 = 0 & \text{on } p = 0, \\ h = 0 & \text{on } p = p_0, \end{cases} \tag{2.3}$$

in the fixed rectangle $R = (-L, L) \times (p_0, 0)$ where $h(q, p) = y + d$ is even and has period $2L$ in the q-variable. We take $q = x = 0$ to correspond to the crest and $q = x = L$ the trough. The height h above the flat bed satisfies

$$h_q = \frac{v}{u-c}, \qquad h_p = \frac{1}{c-u}.$$

The coordinate transformation $(x, y) \to (q, p)$ is global because of (2.2). The evenness of h reflects the requirement that u and η are symmetric while v is antisymmetric around the line AB located strictly below the wave crest. Any solution with a free surface S that is monotone between crest and trough has to be symmetric [13,14]. The transformation (2.3) leads to the formulas

$$\partial_q = \partial_x - \frac{v}{c-u}\partial_y, \quad \partial_p = \frac{1}{c-u}\partial_y, \quad \partial_x = \partial_q - \frac{h_q}{h_p}\partial_p, \quad \partial_y = \frac{1}{h_p}\partial_p.$$

Working with the reformulation (2.3) of the water-wave problem and using bifurcation and degree theory, the existence of a global connected set $\mathcal{C}$ of smooth solutions was proven in [12], for any $p_0 < 0$, $c > 0$, and smooth γ. This continuum $\mathcal{C}$ contains waves with the value of u at some point u arbitrarily close to the wave speed c. A point where $u(x, y) = c$ is a stagnation point.

In [15] we proved a number of facts concerning the location of the points of maximal horizontal velocity for waves with nonzero vorticity. Such a point is the point in the fluid closest to stagnation because u is everywhere less than c. It might be on the surface or the bottom or somewhere inside. We consider any wave with the properties indicated above; this includes all the waves in $\mathcal{C}$. To avoid trivialities, we exclude the waves with completely flat surfaces $\eta'(x) \equiv 0$. *The vorticity function γ is arbitrary unless otherwise stated.*

(i) *There is no interior point of maximal horizontal velocity if $\gamma' \geqslant 0$.*

(ii) *If a point of maximal horizontal velocity lies on the bed, then it is the point B directly below the crest.* The function

$$f = \frac{1}{2}(c-u)^2 - \Gamma(-\psi),$$

where $\Gamma(p) = \gamma(-p)$, $\Gamma(0) = 0$, has certain monotonicity properties. Let us denote by A the wave crest $(0, \eta(0))$, by B the point $(0, -d)$ located on the bed directly below the wave crest, and by C the point $(L, -d)$ located on the bed directly below the wave trough $D = (L, \eta(L))$. Then

(iii) *The function f is strictly increasing on the segments from A to B, B to C, and C to D.*

(iv) *In terms of the* (q, p) *coordinates,*

$$\frac{\partial f}{\partial q} = P_x \quad \text{and} \quad \frac{\partial f}{\partial p} = -v_x.$$

(v) *Any point* J *of maximal horizontal velocity on the top surface* S *satisfies the inequality*

$$v^2(J) \geqslant 2g\big[\eta(A) - \eta(J)\big].$$

(vi) *The trough* D *can never be a point of maximal horizontal velocity (unless* S *is flat).*

(vii) *Consider the restriction of* $c - u$ *to the vertical segment* AB *directly below the crest.*

(a) *If* $\gamma \leqslant 0$ *then* $c - u$ *is strictly monotone on* AB *with its minimum at the crest* A.

(b) *If* $\gamma > 0$ *then* $c - u$ *has a local minimum at the point* B *on the bed.*

(c) *If* $\gamma > 0$ *is sufficiently small and if the solutions depend continuously on* γ, *then* $c - u$ *has a local minimum at the crest* A *as well as at* B.

(viii) *If* $\gamma \leqslant 0$ *then no point of maximal horizontal velocity can lie on the bed.*

(ix) *If the pressure* $P(x, y)$ *throughout the fluid is larger than atmospheric pressure* P_{atm}, *then any point of maximal horizontal velocity on the free surface* S *must be the crest* A.

(x) *Given* $p_0 < 0$, *assume that* $\gamma \leqslant 0$ *is a constant that satisfies*

$$g^2 \geqslant 2g\sqrt{2p_0\gamma^3} + 2\gamma^3 p_0.$$

Then for every wave in the continuum of solutions $\mathcal{C}$ *the point of maximum horizontal velocity must be the wave crest* A. (*Since* $p_0 < 0$, *this inequality holds for* $\gamma \leqslant 0$ *if* $|\gamma|$ *is small enough. In the irrotational case* $\gamma = 0$, *one recovers the classical result* [16,17] *that was originally obtained by complex-analytical methods specific to irrotational flows.*)

All these facts are proven in [15]. Note however that the precise locations of the points of maximal horizontal velocity are not completely determined by this theoretical analysis. This was an important motivation for the present study.

3. Simulation

The goal of our simulation is to further investigate the qualitative properties of the steady waves along the continuum $\mathcal{C}$ for arbitrary vorticities. Our primary motivation is to investigate the extreme waves, that is, the waves that possess points of stagnation. So, as we move along $\mathcal{C}$, we look for the first point along $\mathcal{C}$ where $u = c$ at some point in the domain. The transformed equation given by (2.3) provides a tractable formulation for numerical simulations. Note that under condition (2.2), the PDE is elliptic. The computational domain, the rectangle R, is partitioned into equal rectangular cells where the number of cells is variable and is determined by convergence criteria. M refers to the number of grid points along the p-axis and N to that along the q-axis. Eq. (2.3) is discretized by finite-differencing to yield a system of nonlinear algebraic equations involving the numerical value of u at each gridpoint and, for the equations governing the top boundary, the value of Q. We use central differences for the terms h_{pp} and h_{qq} and approximate the mixed derivative h_{pq} as

$$h_{pq} = \frac{1}{4\Delta p\,\Delta q}(h_{i+1,j+1} - h_{i-1,j+1} - h_{i+1,j-1} + h_{h-1,j-1}).$$

For fixed Q, this system can be solved by a Newton iteration.

To effectively calculate waves along $\mathcal{C}$, we linked our code to two packages, LOCA (a Library of Continuation Methods) and NOX (an Object-Oriented Nonlinear Solver), both of which are part of a more comprehensive numerical software package TRILINOS written in C++ and under development at Sandia National Laboratories. The main component of LOCA is their stepper class which repeatedly calls the nonlinear solver in NOX at each point along the bifurcation curve. The stepper class in turn relies on a large number of support classes for continuation. In addition to providing a discretization of (2.3) and the associated Jacobian (which we derived analytically and then discretized), we inserted numerous customized routines fine-tuned several key parameters to calculate the waves along the continua with accuracy and efficiency. The customized routines included efficient non-graphical checks for other qualitative

behavior such as turning points and secondary bifurcations along the continuum. The fine-tuning of the parameters – primarily the convergence tolerances for the linear and nonlinear solvers – was especially important for our application since our primary interest was to continue up to stagnation. Near stagnation, the Jacobian becomes nearly singular resulting in a large condition number. We use a GMRES solver together with an ILU preconditioner to ensure that the tolerance to condition number ratio yields at least four digits of accuracy.

For a given vorticity function γ, the first step in our procedure is to locate the value Q^* along the trivial curve from which a known bifurcation curve arises. Analytically, this requires us to solve a differential equation, which in turn determines the corresponding trivial solution which is found by solving an integral equation in γ and Q^*. Numerically, we solve this differential equation using an off-the-shelf implicit ODE solver in the TRILINOS package and then use a backward trapezoidal method to solve the integral equation for the corresponding trivial solution. These initial guesses of Q^* and of the corresponding trivial solution are made in the form of an $MN+1$ vector. Convergence onto the trivial curve, for typical choices of grid size $M = N = 250$ or $M = 250$, $N = 500$, is usually attained in fewer than three iterations. Once on the trivial curve, the program proceeds to track along the trivial curve and stops upon a change in sign of an eigenvalue. For the case of constant vorticity, the differential equation that determines a point of bifurcation reduces to an implicit equation, which can be rapidly solved using a fast Newton iteration-based nonlinear solver. For values of γ in the range $-4 \leqslant \gamma \leqslant +10$, only a slight change in Q of order $\mathrm{O}(10^{-3})$ – is observed between the converged guess and the point Q^* at which a zero eigenvalue is detected.

Once Q^* is found, we get onto the bifurcation curve $\mathcal{C}$ by providing the program an approximate solution by shooting in the direction of the eigenvector associated to the zero eigenvalue. Simple, nongraphical, diagnostics are put in place to ensure that we are no longer on the trivial curve. Once on the bifurcation curve $\mathcal{C}$, the continuation proceeds. Checks are made for the size of $c - u$ at appropriate points in the domain R, as well as for turning points and secondary bifurcations.

Restricting our attention now to constant vorticity, we report on several noteworthy properties of waves generated through our simulations. Chief amongst these concerns the location of the first point of stagnation along the bifurcation curve and the shape of the wave near stagnation. Our simulation never actually generates waves with stagnation points since the equation given by (2.3) becomes degenerate elliptic when $u = c$ which is reflected in a singular Jacobian in our discretization. The determination of when a point is considered stagnant, then, cannot simply be made based on the value of $c - u$ since this will never be identically zero. Our determination for first points of stagnation is a combination of a careful calibration of the convergence tolerances for the linear and nonlinear solvers as well as a percentage decrease in the value of $c - u$ relative to its value at the bifurcating point on the trivial curve. This calibration was based on extensive runs for the irrotational case, a case for which much more is known. For each grid size, we set convergence tolerances in order to avoid the program continuing to track along the bifurcation curve yielding "solutions" with numerical artifacts like spiky or plateaued crests. Additionally, for the purpose of determining which waves are nearly stagnant, we require that the minimum value of $c - u$ be less than ten percent of its value at the initially bifurcating wave.

The choice of mesh size was based on the preliminary checks that we made comparing the cases of $M = N = 150$, $M = N = 250$, $M = 250$, $N = 500$ and $M = N = 500$. The location of stagnation point remained the same for these choices of mesh size, and the percentage change in the location of the bifurcation point and the amplitude of the nearly stagnant waves from each resolution to the next finer one decreased. Changes in N are more critical than changes in M, especially for good resolution of streamlines. So, we have based results shown in the next section on runs for $M = 250$, $N = 500$. For the sake of visibility, all figures of waves except Fig. 12 are printed with only every ten streamlines shown.

4. Results

One of our key observations is that given p_0, the relative mass flux, and $2L$, the period of the wave, there is a critical value γ_{crit} of the vorticity that separates the cases for which the first stagnation occurs at the crest or on the bottom. The streamlines are level curves of the velocity potential ψ. Vertical separation of two nearby streamlines occurs where $\psi_y = u - c$ is small, that is, near a stagnation point. In this paper, we always use the normalizations $L = 2\pi$, $p_0 = -2$. Our computations show that $2.95 < \gamma_{\mathrm{crit}} < 3.00$.

These results are in general agreement with those of [2], in that we find cases for which the first stagnation occurs at the crest A and cases for which it occurs on the bottom at B. They however did not make a systematic study to distinguish when these two cases occurred.

Our results are consistent with the analytical results given by (i)–(x) in Section 2, which will be referred to throughout this section. While we did not assume that stagnation could occur only at the crest A and the point B on the bottom just below the crest, we in fact found that our simulations produced only these two locations on the boundary as points of stagnation. The result of (i) furthermore provides good insight to construct a variable vorticity distribution with an internal point of stagnation.

In the course of many runs, we made various checks for other qualitative features of the continuum $\mathcal{C}$ itself. We saw many turning points but never saw any secondary bifurcations. This does not, however, preclude the existence of secondary bifurcations that we might have missed.

4.1. Supercritical constant vorticity

For $\gamma > \gamma_{\text{crit}}$, the first stagnation occurs on the bottom at the point B directly below the crest. This is in direct contrast with the well-studied irrotational case, for which stagnation only occurs at the crest. This point B was also analytically shown in (ii) to be the only candidate for stagnation if stagnation were to occur on the bed. Since our formulation only permits waves with streamlines which are graphs, we never see actual eddies form as in the case of [2]; however, we do see the separation of streamlines and can measure the value of $c - u = 1/h_p$ at any point. A typical case given by $\gamma = 3$ is shown in Fig. 2. The left column illustrates the streamlines of four of the waves occurring along the continuum. The first picture is the trivial wave from which $\mathcal{C}$ bifurcates, while the fourth picture is the "extreme" wave near stagnation. The separation of the streamlines from the bottom near the point B directly under the crest indicates that a stagnation point is forming at B.

This is corroborated by the plots of $c - u$ versus the depth along the vertical crest-bottom line AB in the right column of Fig. 2. The bottom is a local minimum for each of these plots (and in fact for every such plot along the continuum), consistent with what was analytically proven in (vii)(b). There is a very sudden drop of $c - u$ only very near the bottom B near stagnation; the relevant region is magnified in Fig. 3. That is, only the point right next to the bottom is near stagnation. This is the case for both our runs made for $M = 250$, $N = 500$ and $M = N = 500$, which suggests the presence of a very thin boundary layer.

On the other hand, horizontally along the bottom the values of $c - u$ change rather gradually near the stagnation point, as is seen in Fig. 4. That is, the points on the bottom that are near B are also rather near stagnation. The presence of a first point of stagnation at the bottom further elucidates the picture provided by [2] using the method of pseudo-stream functions, who show that waves with eddies, waves that are well beyond the first point of stagnation and have developed several points of stagnation, form near the bottom.

For quite large positive constant vorticity, the same general properties are valid, except that stagnation on the bottom occurs much earlier along the bifurcating curve $\mathcal{C}$. Fig. 5 illustrates two waves of $\mathcal{C}$ in the case $\gamma = 10$. While the graph of $c - u$ below the crest is still monotonically decreasing from A to B, the value of $c - u$ at the crest remains nearly fixed as we continue along $\mathcal{C}$, in contrast to the case $\gamma = 3$, where the value of $c - u$ at the crest experiences a significant drop along $\mathcal{C}$. Note also that stagnation at the bottom occurs so rapidly, as one travels along $\mathcal{C}$, that the surface profile has not had a chance to develop to a significant amplitude. As a result, the maximum amplitude of the wave with a stagnation point in fact decreases as a function of γ, for $\gamma > \gamma_{\text{crit}}$.

4.2. Subcritical constant vorticity

For $\gamma < \gamma_{\text{crit}}$, the first stagnation occurs at the crest, which is consistent with (i) and (viii). The best-studied example is the irrotational case $\gamma = 0$. We include in Fig. 6 the celebrated (irrotational) Stokes wave, the limiting wave of $\mathcal{C}$, with a sharp 120° angle at the crest.

Our computations have further shown that the subcritical interval $\gamma < \gamma_{\text{crit}}$ is naturally subdivided into two subintervals. For the case $0 < \gamma < \gamma_{\text{crit}}$, there is a competition between the crest and the bottom as to which one will approach stagnation first, with the result being that the crest eventually wins out. In case $\gamma \leqslant 0$ the crest is the clear candidate from beginning to end.

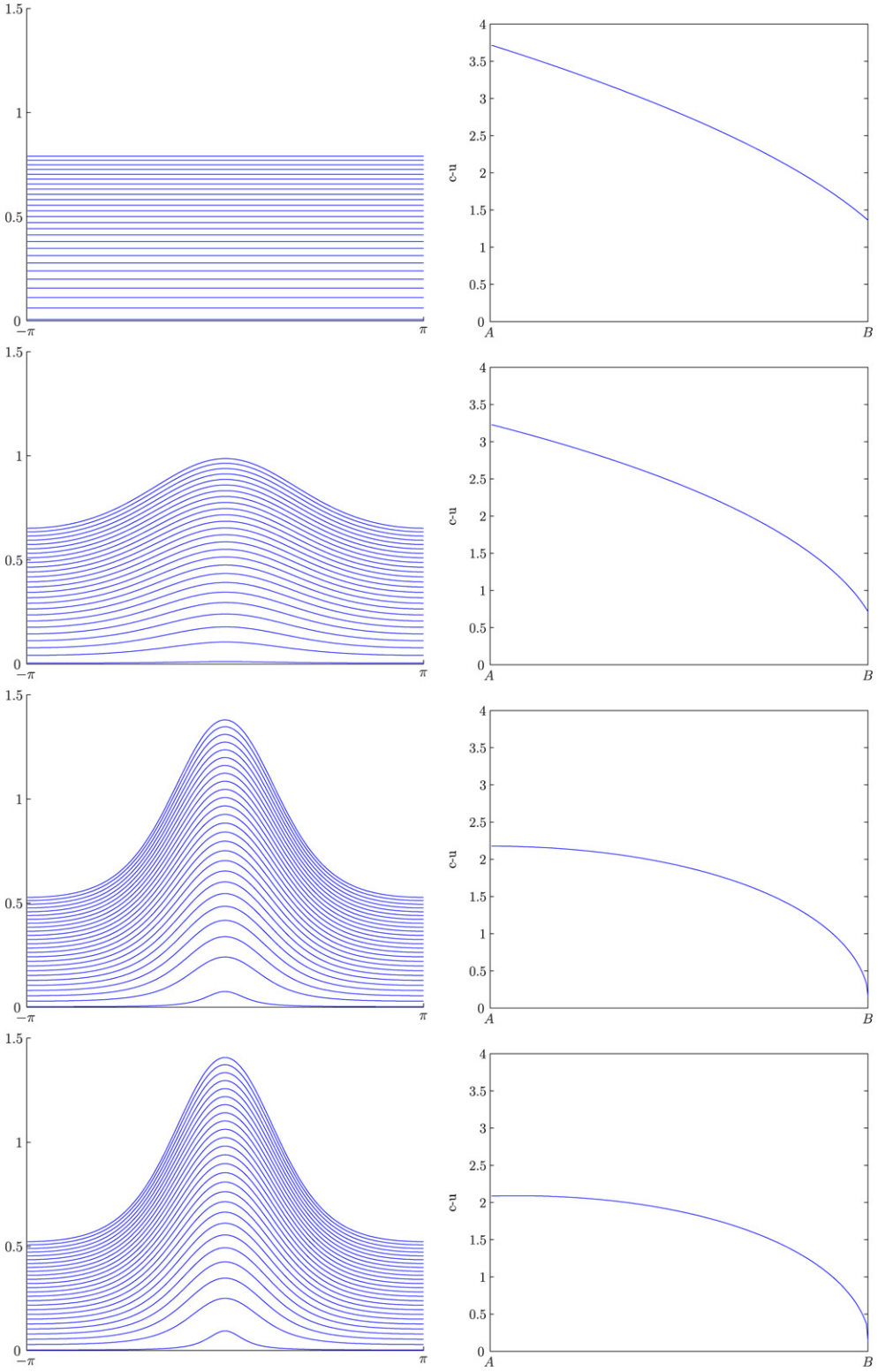

Fig. 2. Four waves along the continuum for $\gamma = 3$. Left: profiles along streamlines. Right: $c - u$ along the line directly below the crest AB.

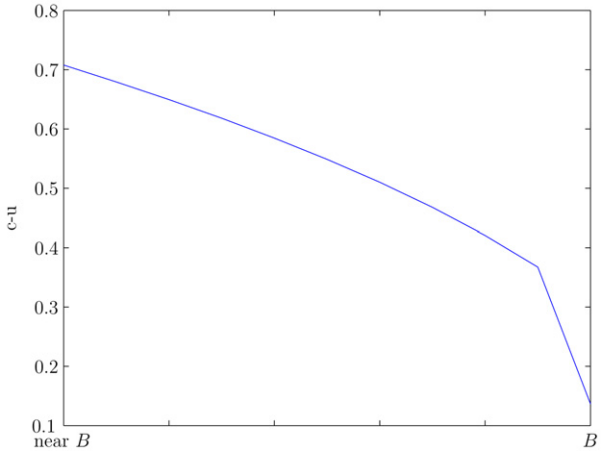

Fig. 3. $\gamma = 3$. Blowup of $c-u$ directly below the crest near the bottom for the wave near stagnation shown in the last row of Fig 2.

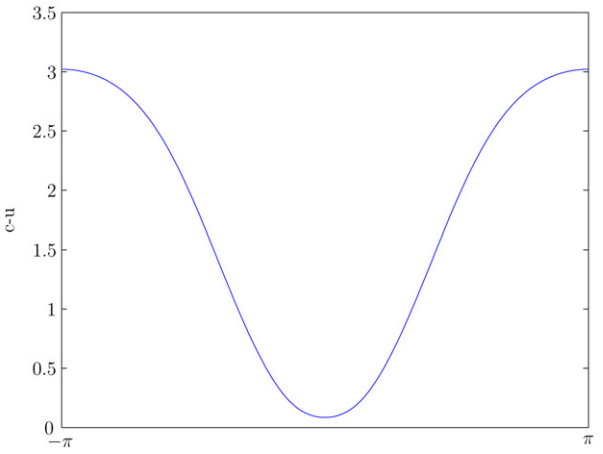

Fig. 4. $\gamma = 3$. $c-u$ along the bottom for the wave near stagnation shown in the last row of Fig. 2.

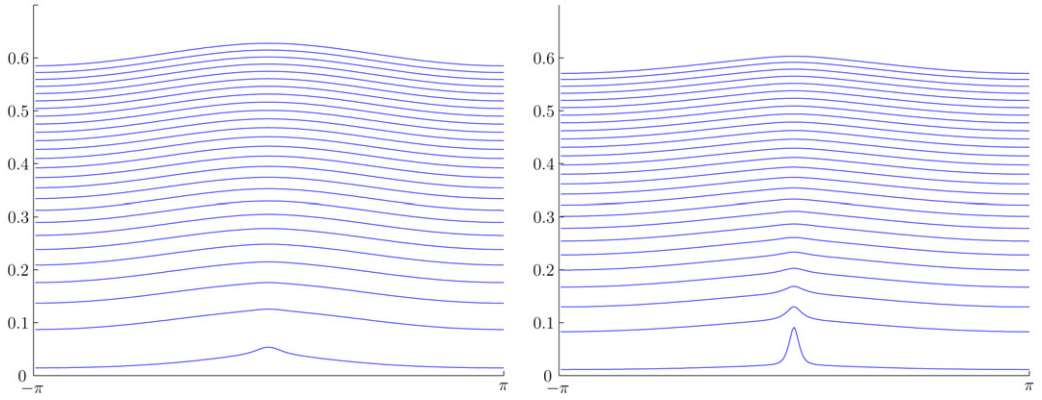

Fig. 5. $\gamma = 10$.

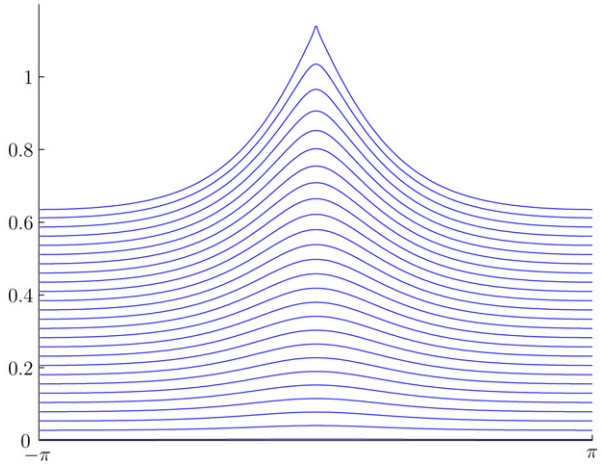

Fig. 6. $\gamma = 0$. Stokes' wave.

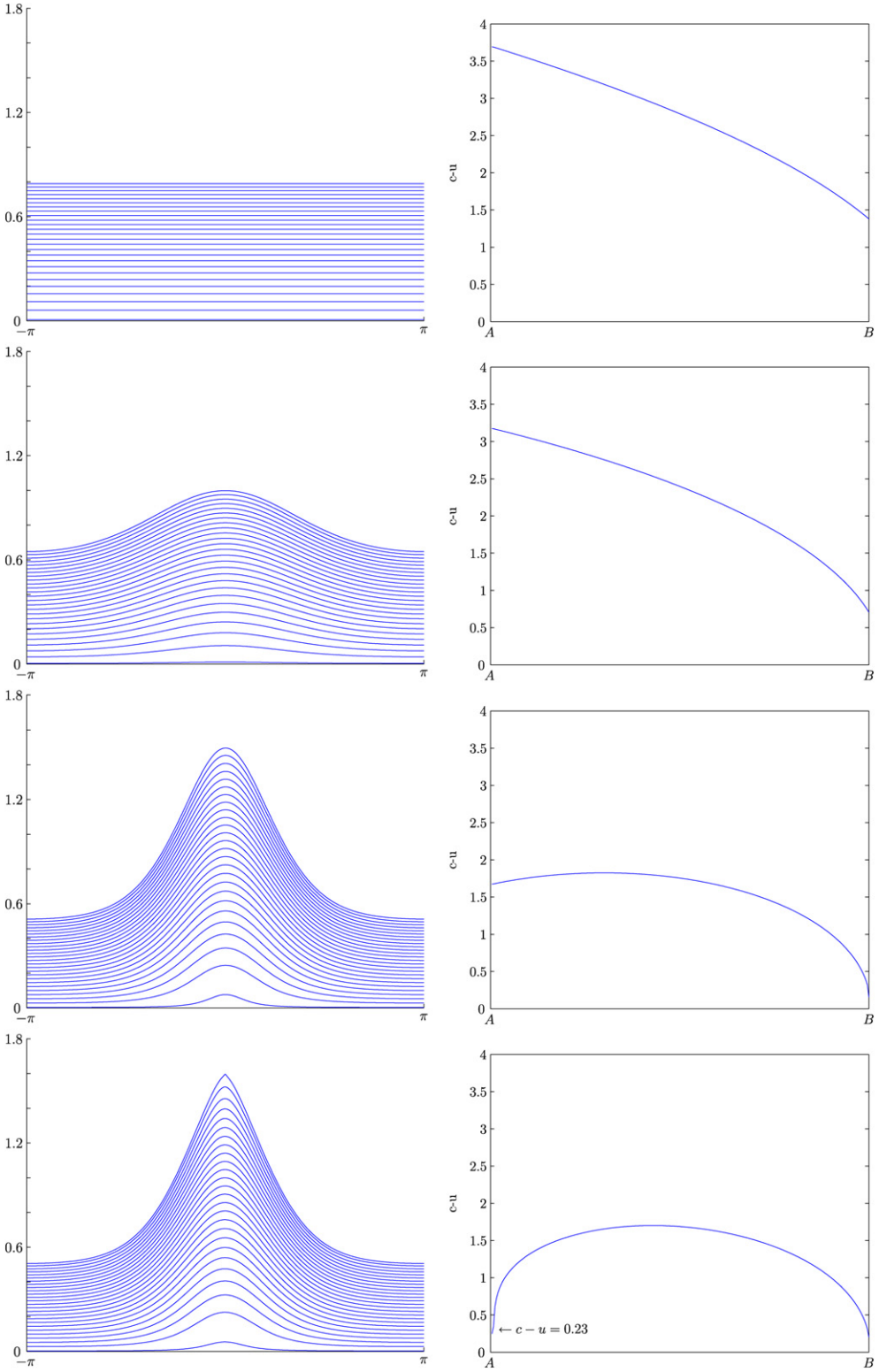

Fig. 7. $\gamma = 2.95$.

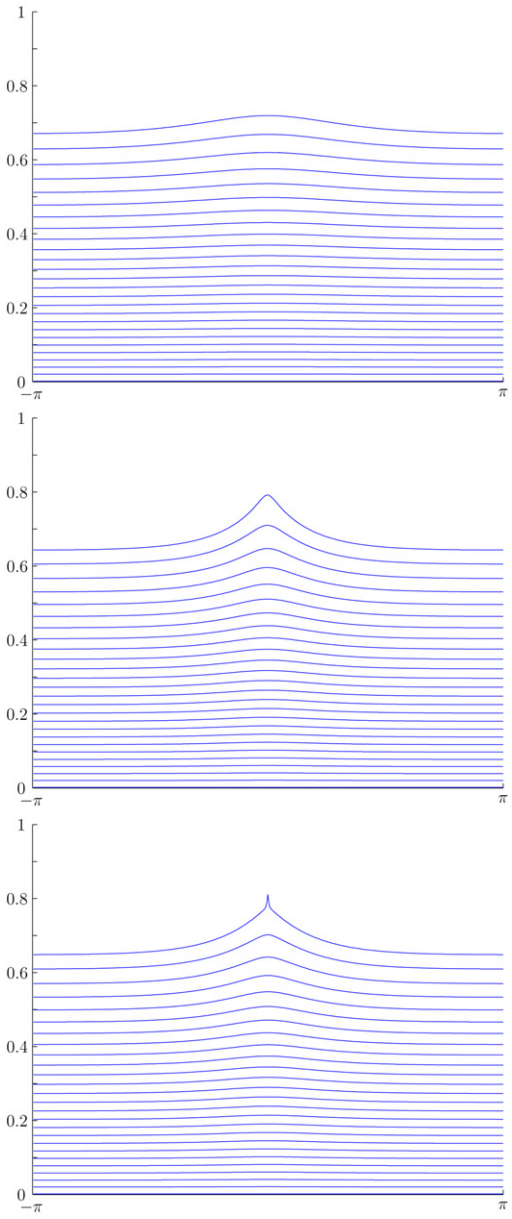

Fig. 8. $\gamma = -4$.

A case in the interval of subcritical positive vorticity is given by $\gamma = 2.95$. The left column of Fig. 7 illustrates the streamlines of four of the waves occurring along the continuum. The first picture is the trivial wave from which $\mathcal{C}$ bifurcates, while the fourth picture is near stagnation. There is a competition between the crest and the bottom as to which one will win out. Although we can see some separation of the streamlines near the bottom, at the very end the crest is the point that finally wins the battle for stagnation. This is difficult to discern from the streamlines but can be more clearly seen from the right column of Fig. 7, which are the graphs of $c - u$ versus depth along the line AB. Although subtle, notice that the value of $c - u$ at the bottom steadily decreases and then increases a bit from the third to the last row, while the value of $c - u$ at the top monotonically decreases to stagnation. Moreover, the ratio of the value of $c - u$ at the bottom near stagnation (last row) to that of the trivial curve (first row) never actually reaches 0.1, which is our criterion for identifying nearly stagnant points. The lack of monotonicity of $c - u$ on the line AB seems to be a property shared by all the waves with points of near stagnation in the range $0 < \gamma < \gamma_{\text{crit}}$. The fact that the

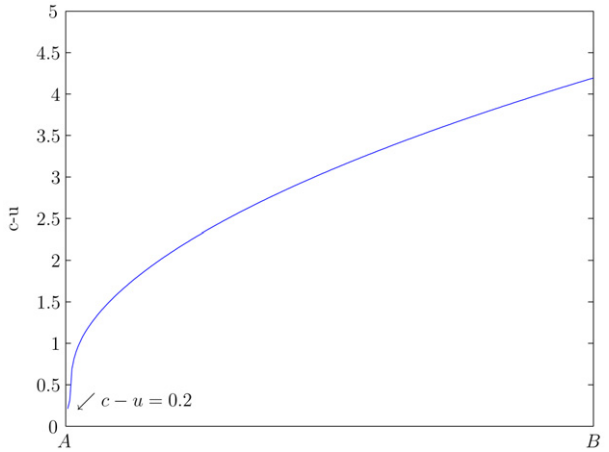

Fig. 9. $\gamma = -4$. $c - u$ along the vertical line AB for the wave near stagnation shown in the last row of Fig. 8.

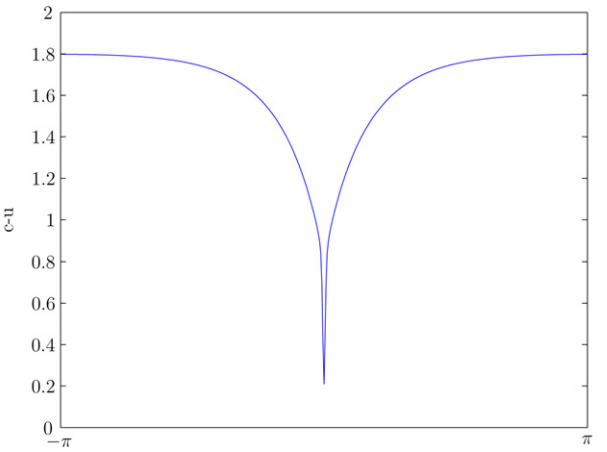

Fig. 10. $\gamma = -4$. $c - u$ along the free surface S for the wave near stagnation shown in the last row of Fig. 8.

bottom is not a minimum especially near stagnation corroborates the analytical results – particularly (vii)(b) – since B is indeed a local minimum. One should also compare the wave near stagnation for $\gamma = 2.95$ in Fig. 7 with that for $\gamma = 3$ in Fig. 2.

For negative vorticity, we find that for all the runs we made, the only point of stagnation is the crest. The only analytical result in this vein is for small negative vorticity as stated in (x). The points between the crest and the trough on the free surface have not analytically been eliminated as candidates for stagnation in this case. However, our simulations support the analytic conjecture that the crest is the only point of stagnation for all negative vorticity.

The only case we show here is a significantly negative vorticity, $\gamma = -4$. Three pictures of waves along the continuum $\mathcal{C}$ are shown in Fig. 8. The profile of the free surface develops like the irrotational case, in the sense that the crest suffers no competition at all from the bottom. Fig. 9 shows $c - u$ on the vertical line AB corresponding to the last wave in Fig. 8. This graph is monotonically decreasing from A to B all along $\mathcal{C}$, in agreement with (vii)(a). For such a negative vorticity, the nearly stagnant wave has a very wide trough and the crest becomes quite sharp. Additionally, the stagnation occurs so rapidly that the amplitude grows only a little along $\mathcal{C}$ and changes very little while the crest sharpens. Fig. 10 shows that the stagnation occurs only extremely near the crest; at any significant distance from the crest, there is no stagnation. The contrast between Figs. 10 and 4 indicates a very different horizontal effect.

In Fig. 11 we compare the surface profiles of the waves near stagnation as a function of γ for four subcritical cases $\gamma = -4, -2, 0, 2.95$. (We have also run several intermediate cases.) As γ decreases, there are several consistent changes:

- The amplitude of the crest decreases.
- The shape of the wave near the crest goes from concave to convex. The crest becomes sharper.
- The trough becomes wider and flatter (greater crest-trough asymmetry).
- The depth of the trough increases from $\gamma = 2.95$ to -2, but decreases slightly from $\gamma = -2$ to -4.
- The value of Q corresponding to the stagnant wave decreases as a function of γ. The Q values are 32.2406, 22.4803, 18.6145 and 15.9659.

4.3. Variable vorticity

The DJ transformation and hence our simulations permit nonconstant vorticity distributions, which opens the door to investigating more realistic flows than those with constant vorticity. A class of vorticity distributions that are particularly flexible are step functions which potentially can model water waves propagating on currents or surface shears generated by wind. A systematic study of the effect of variable vorticity distributions on the qualitative properties of extreme waves will follow in a subsequent paper. We show here only one case of a flow with a vorticity distribution which, although slightly contrived, results in an internal point of stagnation. Such a point cannot occur for any distri-

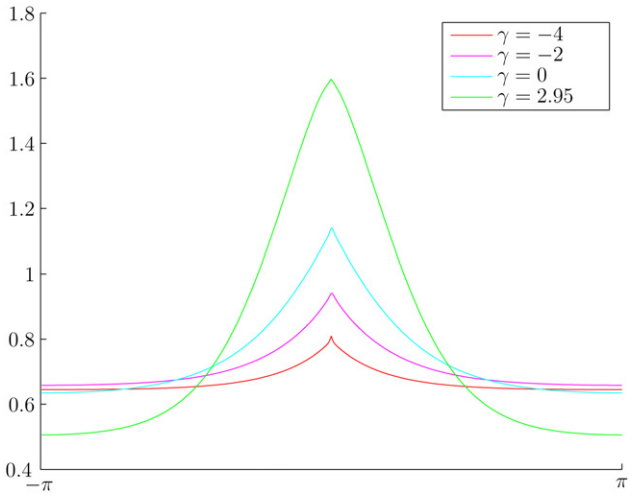

Fig. 11. Waves near stagnation for four subcritical values of γ.

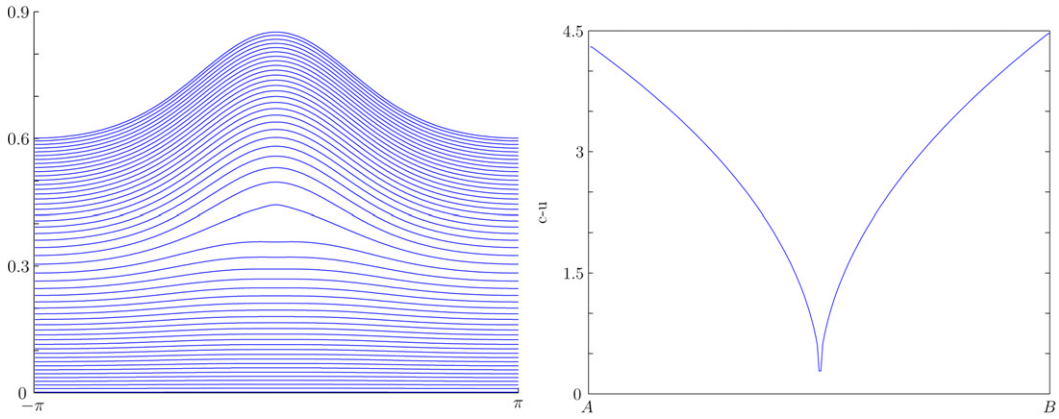

Fig. 12. Internal stagnation.

bution satisfying $\gamma' \leqslant 0$ as proved in (i). Therefore, a simple choice for a vorticity distribution that could conceivably yield an internal stagnation is an increasing step function. For fixed $p_0 = -2$, we choose γ to be

$$\gamma(p) = \begin{cases} -10, & -2 < p < -1, \\ 10, & -1 < p < 0. \end{cases} \tag{4.1}$$

Fig. 12 shows the streamlines of the wave near stagnation corresponding this choice of vorticity as well as the plot of $c - u$ on AB. Indeed we see an internal stagnation point.

Acknowledgements

Several people were crucial to the success of this project. Our computer wizard, Joshua Bronson, set up the interface with Trilinos for us. Andrew Salinger of Sandia National Laboratories generously lent us his expertise concerning Trilinos and numerical bifurcation. Adrian Constantin has been a close collaborator on the analytical aspects of water waves.

References

[1] J.A. Simmen, P.G. Saffman, Steady deep-water waves on a linear shear current, Stud. Appl. Math. 73 (1) (1985) 35–57.

[2] A.F. Teles da Silva, D.H. Peregrine, Steep, steady surface waves on water of finite depth with constant vorticity, J. Fluid Mech. 195 (1988) 281–302.
[3] J.-M. Vanden-Broeck, Steep solitary waves in water of finite depth with constant vorticity, J. Fluid Mech. 274 (1994) 339–348.
[4] J.-M. Vanden-Broeck, New families of steep solitary waves in water of finite depth with constant vorticity, Eur. J. Mech. B Fluids 14 (6) (1995) 761–774.
[5] H. Okamoto, M. Shōji, The Mathematical Theory of Permanent Progressive Water-Waves, Advanced Series in Nonlinear Dynamics, vol. 20, World Scientific Publishing Co. Inc., River Edge, NJ, 2001.
[6] V.A. Miroshnikov, The Boussinesq–Rayleigh approximation for rotational solitary waves on shallow water with uniform vorticity, J. Fluid Mech. 456 (2002) 1–32.
[7] R.A. Dalrymple, A numerical model for periodic finite amplitude waves on a rotational fluid, J. Comput. Phys. 24 (1) (1977) 29–42.
[8] M.-L. Dubreil-Jacotin, Sur la détermination rigoureuse des ondes permanentes périodiques d'ampleur finie, J. Math. Pures Appl. 13 (1934) 217–291.
[9] G.P. Thomas, Wavecurrent interactions: an experimental and numerical study. Part 2. Nonlinear waves, J. Fluid Mech. 216 (1990) 505–536.
[10] T. Brooke Benjamin, The solitary wave on a stream with an arbitrary distribution of vorticity, J. Fluid Mech. 12 (1962) 97–116.
[11] C. Swan, I.P. Cummins, R.L. James, An experimental study of two-dimensional surface water waves propagating on depth-varying currents. Part 1. Regular waves, J. Fluid Mech. 428 (2001) 273–304.
[12] A. Constantin, W. Strauss, Exact steady periodic water waves with vorticity, Comm. Pure Appl. Math. 57 (4) (2004) 481–527.
[13] A. Constantin, J. Escher, Symmetry of steady deep-water waves with vorticity, Eur. J. Appl. Math. 15 (6) (2004) 755–768.
[14] V.M. Hur, Symmetry of steady periodic surface water waves with vorticity, Philos. Trans. Roy. Soc. (2007), in press.
[15] A. Constantin, W. Strauss, Rotational steady water waves near stagnation, Philos. Trans. Roy. Soc. (2007), in press.
[16] J.F. Toland, On the existence of a wave of greatest height and Stokes's conjecture, Proc. Roy. Soc. London Ser. A 363 (1715) (1978) 469–485.
[17] J.F. Toland, Stokes waves, Topol. Methods Nonlinear Anal. 7 (1) (1996) 1–48.